Disease Models & Mechanisms 3, 743-751 (2010) doi:10.1242/dmm.004002

Genetic and chemical modulation of spastin-dependent axon outgrowth in zebrafish embryos indicates a role for impaired microtubule dynamics in hereditary spastic paraplegia

Richard Butler[1,*,‡], Jonathan D. Wood[1,2,*,§], Jennifer A. Landers[1] and Vincent T. Cunliffe[1,§]

SUMMARY

Mutations in the *SPAST* (*SPG4*) gene, which encodes the microtubule-severing protein spastin, are the most common cause of autosomal dominant hereditary spastic paraplegia (HSP). Following on from previous work in our laboratory showing that spastin is required for axon outgrowth, we report here that the related microtubule-severing protein katanin is also required for axon outgrowth in vivo. Using confocal time-lapse imaging, we have identified requirements for spastin and katanin in maintaining normal axonal microtubule dynamics and growth cone motility in vivo, supporting a model in which microtubule severing is required for concerted growth of neuronal microtubules. Simultaneous knockdown of spastin and katanin caused a more severe phenotype than did individual knockdown of either gene, suggesting that they have different but related functions in supporting axon outgrowth. In addition, the microtubule-destabilising drug nocodazole abolished microtubule dynamics and growth cone motility, and enhanced phenotypic severity in *spast*-knockdown zebrafish embryos. Thus, disruption of microtubule dynamics might underlie neuronal dysfunction in this model, and this system could be used to identify compounds that modulate microtubule dynamics, some of which might have therapeutic potential in HSP.

INTRODUCTION

The hereditary spastic paraplegias (HSPs) are a collection of neurodegenerative disorders characterised by progressive lower-limb spasticity and caused by the developmental failure or degeneration of upper motor axons in the corticospinal tract (Crosby and Proukakis, 2002; Reid, 2003). Mutations in the *SPAST* gene (also known as *SPG4*) are the most common cause of autosomal dominant HSP, and spastin (the *SPAST* gene product) is a microtubule-severing ATPase (Evans et al., 2005; Roll-Mecak and Vale, 2005; Salinas et al., 2005) that shares sequence and functional similarity with the p60 subunit of katanin (P60-katanin). Genetic and biochemical studies have demonstrated that *SPAST* mutations cause loss of spastin function, making haploinsufficiency a likely disease mechanism (Charvin et al., 2003; Evans et al., 2005; Patrono et al., 2002), although dominant-negative effects could contribute to disease pathogenesis in some cases (Errico et al., 2002; McDermott et al., 2003). To investigate the developmental requirements for spastin, we previously used morpholino antisense methods to knockdown *spast* expression in the zebrafish embryo and demonstrated a crucial requirement for spastin to promote axon outgrowth during embryonic development (Wood et al., 2006).

[1]MRC Centre for Developmental and Biomedical Genetics, Department of Biomedical Science, University of Sheffield, Sheffield, S10 2TN, UK
[2]Department of Neuroscience, School of Medicine and Biomedical Sciences, Sheffield, S10 2RX, UK
*These authors contributed equally to this work
‡Present address: Wellcome Trust Sanger Institute, Hinxton, Cambridge, CB10 1SA, UK
§Authors for correspondence (j.d.wood1@sheffield.ac.uk; v.t.cunliffe@sheffield.ac.uk)

SPAST HSP cases are characterised by variability in the age of onset both between and within pedigrees (Durr et al., 1996), suggesting that other factors are important in defining disease severity. Similar to the function that we have shown for spastin in the zebrafish embryo, the microtubule-severing activity of P60-katanin is required to promote axon outgrowth in isolated mammalian sympathetic neurons (Ahmad et al., 1999; Karabay et al., 2004). We therefore hypothesised that P60-katanin might act as a modifier of spastin function in vivo. To address this possibility, we used morpholino antisense methods to determine the effect of reduced P60-katanin activity on axon outgrowth in the zebrafish embryo. We also investigated the effect of simultaneous knockdown of spastin and P60-katanin to give insight into the mechanistic relationship between the functions of these two microtubule-severing proteins.

Given that spastin and P60-katanin are microtubule-severing proteins with known roles in promoting axon outgrowth, we hypothesised that their activities might be required for axonal microtubule dynamics. When fused to green fluorescent protein (GFP), proteins that bind to microtubule plus-ends, such as end-binding protein 3 (EB3), are powerful markers for visualising microtubule growth events in cultured neurons (Stepanova et al., 2003); these proteins have been termed microtubule-plus-end-tracking proteins (+TIPs). We have developed methods for in vivo analysis of axonal microtubule dynamics in the zebrafish embryo using an EB3-GFP fusion protein, and used these methods to investigate the roles of spastin and katanin in axonal microtubule dynamics. We have also utilised this approach to investigate the effects of microtubule-destabilising drugs on axonal microtubule dynamics in zebrafish embryonic neurons. The findings from these studies suggest a model whereby the microtubule-severing

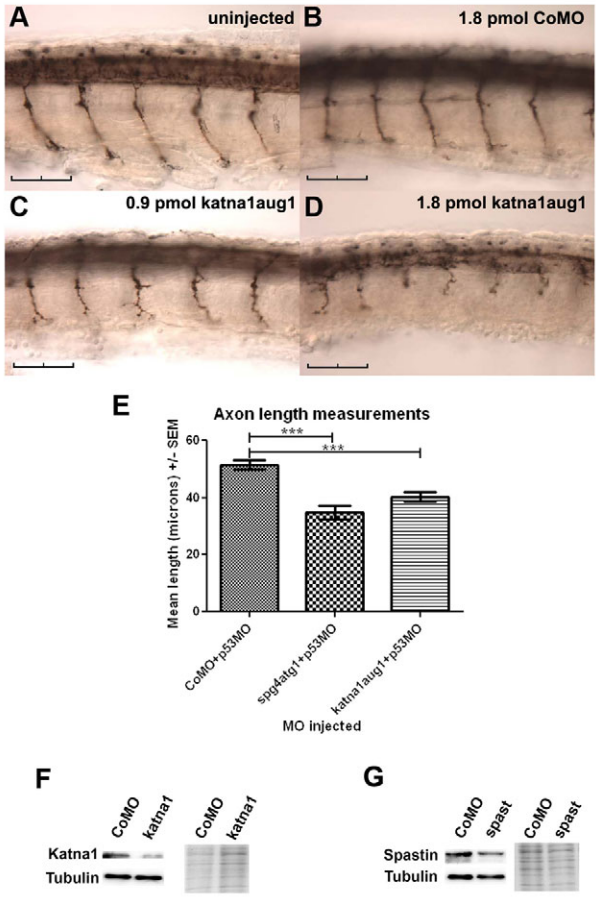

Fig. 1. Morpholino-mediated knockdown of *katna1* function with a translation-blocking (katna1aug1) morpholino inhibits spinal motor axon outgrowth. Embryos were injected with 1.8 pmol of control (CoMO) (B), 0.9 pmol of katna1aug1 (C) or 1.8 pmol of katna1aug1 morpholino (D), fixed at 28 hpf, and then immunostained with znp-1. An uninjected control is shown in A. The effects of *katna1* and *spast* translation-blocking morpholinos on spinal motor axon outgrowth are independent of p53 (E). Axons were measured in embryos injected with 1.0 pmol CoMO + 1.6 pmol p53-specific morpholino (p53MO) (n=20), 0.6 pmol spg4atg1 + 1.2 pmol p53MO (n=21), or 1.0 pmol katna1aug1 + 1.6 pmol p53MO (n=17). Statistical significance was determined using ANOVA with Bonferroni's multiple comparison test. ***P<0.001. (F) Immunoblots for katna1 and tubulin demonstrating that katna1aug1-injected embryos have reduced levels of katna1 protein compared with CoMO-injected embryos. (G) Immunoblots for spastin and tubulin demonstrating that spg4atg1-injected embryos show reduced levels of spastin protein compared with CoMO-injected embryos. The right panel in F and G is a section from an equivalently loaded Coomassie-blue-stained gel to demonstrate relative loadings. Scale bars: 50 μm.

activities of spastin and katanin support the concerted growth of microtubules during embryonic development.

RESULTS

Like spastin, P60-katanin is required for axon outgrowth in the zebrafish embryo

We previously demonstrated a crucial requirement for spastin to promote axon outgrowth in the zebrafish embryo (Wood et al., 2006). Interestingly, the closely related microtubule-severing protein P60-katanin has also been shown to promote axonal growth in cultured primary neurons (Ahmad et al., 1999; Karabay et al., 2004). We therefore hypothesised that the microtubule-severing activity of P60-katanin might also be required for axon outgrowth in the zebrafish embryo. Ensembl (http://www.ensembl.org/index.html) identified ENSDARG00000021827 (zgc:110580) as the zebrafish orthologue of human *KATNA1* (encoding katanin p60 subunit A1), which we refer to here as *katna1*. The predicted protein product of this gene shares 75% identity and 84% similarity with the human KATNA1-201 variant. The human genome also contains two related genes – the p60 katanin subunit A-like genes *KATNAL1* and *KATNAL2* – both of which have predicted zebrafish orthologues (zgc:101696 and zgc:123350, respectively); these zebrafish orthologues share lower similarity with human *KATNA1* than does zgc:110580.

In order to determine whether reduced levels of P60-katanin affect motor axon outgrowth, embryos were microinjected at the one-cell stage either with a morpholino designed to specifically inhibit translation of *katna1* mRNA (katna1aug1) or with a control morpholino (CoMO), and analysed by immunostaining with monoclonal antibody znp-1, which reveals the overall morphology of differentiating spinal motor neurons. This analysis demonstrated that inhibition of *katna1* with katna1aug1 dramatically impaired outgrowth of motor axons from the spinal cord in a dose-dependent manner (Fig. 1A-D; Table 1). The majority of embryos injected with 0.9 pmol katna1aug1 (57.6%, n=97) showed mild defects in spinal motor axon outgrowth, whereas most embryos injected with 1.8 pmol katna1aug1 (91.5%, n=106) showed moderate or severe

Table 1. Quantification of axon outgrowth defects in *katna1*-deficient embryos[a]

	Severity (%)			
Treatment	**0**	**1**	**2**	**3**
Uninjected (n=125)	94.4	4.0	1.6	0
1.8 pmol CoMO (n=99)	62.6	22.2	12.1	3.1
0.9 pmol katna1aug1 (n=97)	11.3	57.6	21.6	8.3
1.8 pmol katna1aug1 (n=106)	0.9	7.5	44.3	47.2
Uninjected (n=57)	100	0	0	0
0.9 pmol CoMO (n=16)	100	0	0	0
1.8 pmol CoMO (n=56)	98.2	0	0	1.8
0.9 pmol katna1e4i4 (n=52)	23.1	40.4	26.9	9.6
1.8 pmol katna1e4i4 (n=63)	7.9	9.5	3.2	79.4

[a]Data pooled from three separate independent experiments for both katna1aug1 and katna1e4i4.

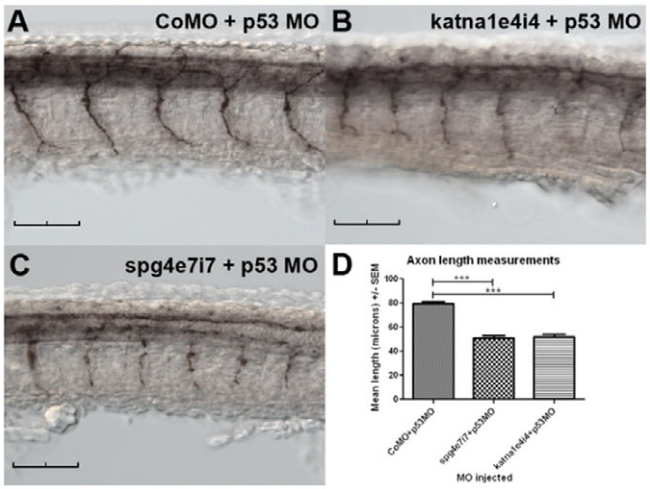

Fig. 2. A *katna1* splice-blocking (katna1e4i4) morpholino inhibits spinal motor axon outgrowth in a p53-independent manner. Embryos were injected with 1.0 pmol CoMO + 1.6 pmol p53MO (A), 0.8 pmol katna1e4i4 + 1.6 pmol p53MO (B) or 1.0 pmol spg4e7i7 + 1.6 pmol p53MO (C), fixed at 28 hpf, and then immunostained with znp-1. Both *katna1* and *spast* splice-blocking morpholinos inhibit spinal motor axon outgrowth in a p53-independent manner (D). CoMO + p53MO (*n*=25), spg4e7i7 + p53MO (*n*=35), katna1e4i4 (*n*=34); statistical significance was determined using ANOVA with Bonferroni's multiple comparison test. ***P<0.001. Scale bars: 50 μm.

defects. Immunoblotting for katna1 and spastin confirmed that the katna1aug1 and spg4atg1 morpholinos reduced katna1 (Fig. 1F) and spastin (Fig. 1G) protein levels, respectively. Similarly, a *katna1* splice-blocking morpholino (katna1e4i4) also inhibited spinal motor axon outgrowth (Fig. 2B) and this effect was dose dependent (Table 1). Reverse-transcriptase polymerase chain reaction (RT-PCR) analysis demonstrated that the severity of the axon outgrowth defects in katna1e4i4 morphants correlated with the appearance of a smaller PCR product and a reduction in the amount of the larger cDNA fragment that was present in the control-injected embryos (supplementary material Fig. S1). These results are consistent with the splice morpholino causing skipping of exon 4, which would give rise to an mRNA encoding a truncated protein comprising a P60-katanin 102-residue N-terminal fragment up to Arg102 followed by a novel 9-residue tail, and lacking residues 103-485. Such a truncated P60-katanin polypeptide would lack the ATPase activity encoded by its AAA domain and thus have either no function or potentially dominant-negative effects.

Some morpholinos can elicit off-target developmental abnormalities in the central nervous system (CNS) of zebrafish embryos through the activation of a p53-dependent cell death pathway (Robu et al., 2007). To ascertain whether the motor axon outgrowth phenotype induced by *katna1* morpholinos was due to such off-target effects, we co-injected a molar excess of a p53-specific morpholino (p53MO) with both *katna1*-specific morpholinos and the control morpholino and measured mean motor axon lengths in znp-1-stained embryos. With 1.0 pmol of katna1aug1 together with 1.6 pmol p53MO, and with 0.8 pmol katna1e4i4 together with 1.6 pmol p53MO, mean axon lengths were 78% and 65%, respectively, of the mean length in embryos injected with 1.0 pmol CoMO together with 1.6 pmol p53MO (Fig. 1E, Fig. 2D). We therefore conclude that reduced levels of *katna1* expression caused spinal motor axon outgrowth defects in vivo. We also demonstrated that the effects of the spg4atg1 and spg4e7i7 morpholinos (Wood et al., 2006) on spinal motor axon outgrowth were independent of p53 (Fig. 1E, Fig. 2C,D). We previously found that *spast* knockdown had widespread effects on axon outgrowth and was not restricted to spinal motor axons. Similarly, the effect of *katna1* knockdown on axon outgrowth was not restricted to spinal motor neurons: reduced znp-1 staining was apparent throughout the spinal cord, suggesting that multiple populations of spinal interneurons were also affected.

P60-katanin and spastin are required for axonal microtubule dynamics

In order to investigate the mechanisms by which the microtubule-severing activities of spastin and P60-katanin promote axon outgrowth, we developed methods for in vivo analysis of microtubule growth events. We constructed the plasmid NBT:EB3-GFP, in which an expression cassette encoding an EB3-GFP fusion protein (Stepanova et al., 2003) was placed under the control of the Xenopus neural-specific β-tubulin (NBT) promoter. Microinjection of this construct into one- to two-cell zebrafish embryos gave a mosaic pattern of GFP expression that was specifically restricted to a scattered population of CNS neurons and more faintly expressing muscle cells, and yielded embryos in which individual EB3-GFP-expressing neurons could be readily visualised and imaged in their normal location within the developing CNS (supplementary material Fig. S2A). At higher magnification, punctate labelling was observed at regular intervals in axons (supplementary material Fig. S2B). Time-lapse confocal imaging demonstrated that these punctate comet-like regions of fluorescence moved in an anterograde direction away from the cell body (supplementary material Fig. S3A and Movie 1). This is clearly illustrated in the kymograph (supplementary material Fig. S3B). Kymography further revealed that the comets moved with a remarkably uniform average velocity of 0.14±0.2 μm/second.

To determine the effect of *spast* and *katna1* knockdown on axonal microtubule dynamics, NBT:EB3-GFP DNA was co-injected into one-cell-stage zebrafish embryos with *spast* and *katna1* translation- and splice-blocking morpholinos, and with control morpholinos (CoMO and spg4CoMO). Time-lapse confocal imaging of axonal EB3-GFP fluorescence was used to monitor microtubule plus-end dynamics (Fig. 3; supplementary material Movies 2-6). Strikingly, in both *spast*-morpholino-injected (Fig. 3B,D) and *katna1*-morpholino-injected (Fig. 3C,E) embryos a near-total loss of discrete puncta of EB3-GFP fluorescence was observed, compared with the situation in control-morpholino-injected embryos (Fig. 3A), where anterograde-moving puncta of fluorescence were observed as in wild-type uninjected embryos. Kymograph analysis revealed that although discrete puncta were absent, a weak anterograde drift of diffuse EB3-GFP fluorescence was still detectable in *spast*- and *katna1*-morphant embryos.

Microtubule-destabilising drugs such as nocodazole and vinblastine have been shown to attenuate synaptic and locomotor phenotypes in Drosophila models of HSP associated with modulation of *Dspastin* activity (Orso et al., 2005; Trotta et al., 2004). We therefore tested whether immersion of zebrafish embryos in media containing these agents modulated outgrowth of spinal

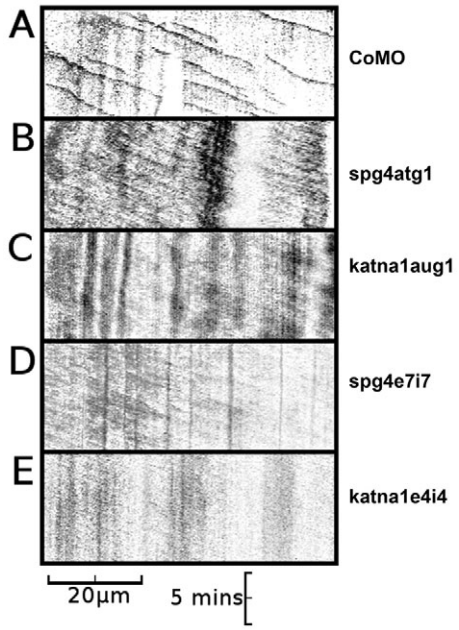

Fig. 3. Axons in *spast* and *katna1* morphants lack discrete EB3-GFP puncta. (A) Kymograph of an axon made from a 10-minute time-lapse recording of a neuron from a CoMO-injected embryo, demonstrating anterograde movement of discrete comet-like puncta of EB3-GFP fluorescence (CoMO, *n*=21; spg4CoMO, *n*=12). (B) Kymograph of an axon made from a 10-minute time-lapse recording of a neuron from a spg4atg1 (0.6 pmol)-injected embryo, demonstrating weak anterograde movement of diffuse GFP fluorescence in the absence of discrete comet-like puncta of EB3-GFP fluorescence (*n*=13). (C) Kymograph of an axon made from a 10-minute time-lapse recording of a neuron from a katna1aug1 (1.8 pmol)-injected embryo, again demonstrating weak anterograde movement of diffuse GFP fluorescence in the absence of discrete puncta of EB3-GFP fluorescence (*n*=10). Equivalent results were obtained with the spg4e7i7 [1.2 pmol; *n*=6; (D)] and katna1e4i4 [1.2 pmol; *n*=6; (E)] morpholinos. Horizontal scale bar: 20 μm, vertical scale bar: 5 minutes. A series of individual frames from each of these time-lapse recordings is shown in supplementary material Fig. S4. See supplementary material Movies 2-6.

motor axons in embryos injected with control and *spast* morpholinos. First, wild-type embryos were exposed continuously to nocodazole at a range of concentrations from 0.1-1.0 μg/ml from 24 hours post-fertilisation (hpf), shortly after the onset of spinal motor axon outgrowth, and then fixed at 30 hpf, towards the end of primary motor axon outgrowth, for immunostaining with znp-1. Over this range of concentrations, nocodazole was found to inhibit axon outgrowth and cause aberrant branching, with a concentration-dependent increase in the severity of the observed outgrowth defects (supplementary material Fig. S5; Table 2). Axons in nocodazole-treated embryos stained robustly with an antibody against acetylated tubulin (results not shown), suggesting that the nocodazole concentrations used do not completely disassemble axonal microtubules. We then tested the effect of the same range of nocodazole concentrations on the axon outgrowth defect caused by reduced *spast* activity, and observed that immersion of *spast*-morphant embryos in embryo medium containing nocodazole enhanced the axon outgrowth defect (Fig. 4; Table 3). Lower doses of nocodazole (0.005-0.05 μg/ml) had no discernible effect on axon outgrowth in either control or morphant embryos (results not shown). Zebrafish embryos were remarkably tolerant of vinblastine such that immersion in medium containing 0.01–10 μM vinblastine had no discernible effect on outgrowth of spinal motor axons or on phenotypic severity in *spast*-morphant embryos (results not shown).

To investigate whether treatment of embryos with nocodazole impaired axonal microtubule dynamics, we exposed NBT:EB3-GFP-injected embryos to nocodazole and performed time-lapse confocal imaging on live anaesthetised embryos (supplementary material Movies 7 and 8). Nocodazole treatment was found to suppress the formation of fluorescent axonal EB3-GFP puncta and to stop all anterograde movement of fluorescent structures (Fig. 5B), in contrast to the situation in DMSO-vehicle-treated control embryos, where vigorous anterograde movement of discrete fluorescent puncta was observed (Fig. 5A).

P60-katanin and spastin are required for growth cone motility

In order to investigate the effects of disrupted microtubule dynamics on the behaviour of growth cones, time-lapse recordings were made of the distal parts of EB3-GFP-expressing neurons in embryos that were injected with *spast* or *katna1* morpholinos, or were treated with nocodazole or DMSO only (supplementary material Movies 9-14). The mean number of outgrowth events per growth cone per minute was calculated from these recordings. Outgrowth events were scored as discrete periods of continuous growth of filopodial processes extending from the growth cone. For those outgrowth events where the process extended for an accurately measurable distance, it was possible to calculate the mean velocity of an outgrowth event by measuring the distance travelled by the tip of the outgrowing process over time. The results of this analysis showed that knockdown of spastin, knockdown of katanin, and treatment of embryos with nocodazole all reduced the number of outgrowth events at growth cones (Fig. 6). These results support the well-established role of normal microtubule function in growth cone motility (Lowery and Van Vactor, 2009),

Table 2. Effect of nocodazole on spinal motor neuron axon outgrowth in wild-type embryos[a]

	Severity (%)			
Treatment	**0**	**1**	**2**	**3**
Untreated (*n*=118)	95.8	3.4	0.8	0
DMSO control (*n*=111)	91.9	6.3	1.8	0
0.1 μg/ml nocodazole (*n*=108)	17.6	80.6	1.8	0
0.3 μg/ml nocodazole (*n*=49)	4.1	73.5	22.4	0
0.5 μg/ml nocodazole (*n*=112)	0.9	37.5	61.6	0
1.0 μg/ml nocodazole (*n*=118)	0	7.6	79.7	12.7

[a]Data pooled from three independent experiments.

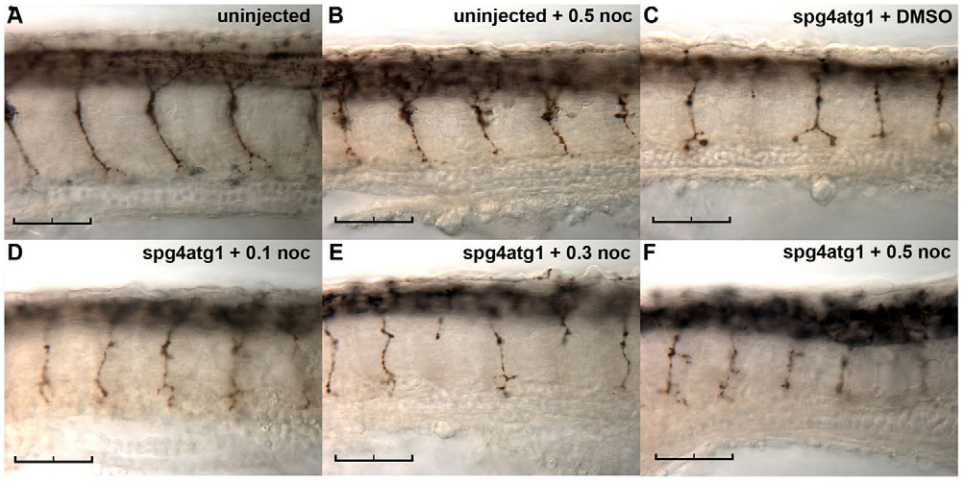

Fig. 4. Nocodazole does not ameliorate the effect of reduced *spast* activity on spinal motor axon outgrowth. Embryos were microinjected with 0.4 pmol of spg4atg1 morpholino and continuously exposed to nocodazole at the concentrations indicated from 24 hpf to 30 hpf, prior to fixation and immunostaining with znp-1. Representative images are shown of an untreated uninjected embryo (A); an uninjected embryo treated with 0.5 µg/ml nocodazole (B); a *spast*-morphant embryo treated with DMSO vehicle (C); a *spast*-morphant embryo treated with 0.1 µg/ml nocodazole (D); a *spast*-morphant embryo treated with 0.3 µg/ml nocodazole (E); and a *spast*-morphant embryo treated with 0.5 µg/ml nocodazole (F). Scale bars: 50 µm.

and reveal a novel, direct role of microtubule severing in control of growth cone activity.

P60-katanin and spastin have different but related functions in axon outgrowth

Having demonstrated that both *katna1* and *spast* functions promote spinal motor axon outgrowth and are required for normal growth cone motility, and given that their protein products have both been shown to possess microtubule-severing activity and promote the growth of microtubule plus-ends along axons, we set out to determine whether these two proteins function in a concerted manner by comparing the effect of simultaneously knocking down both genes with the effect of knocking down either gene individually. We performed a series of titrations that enabled us to establish individual doses of each morpholino that caused only mild to moderate spinal motor axon outgrowth defects when injected into zebrafish embryos: 93.3% (n=104) with 0.3 pmol *spast* morpholino; and 77.7% (n=85) with 0.9 pmol katna1aug1 morpholino. When these morpholinos were simultaneously co-injected at these concentrations, a substantially enhanced phenotype was observed, with 58.3% of embryos (n=96) showing severe defects (Fig. 7; Table 4). These qualitative assessments of phenotypic severity were in accord with quantitative measurements of spinal motor axon length that showed mean axon lengths in *spast* and *katna1* morphants were 72% and 63% of those measured in control-injected embryos, whereas the double morphants showed a further reduction to 26% of that in controls (Fig. 7E).

DISCUSSION

Our finding that *katna1* is required for axon outgrowth in the zebrafish embryo is consistent with previous work demonstrating that katanin is required for axonal growth by mammalian neurons cultured in vitro (Ahmad et al., 1999; Karabay et al., 2004). This functional overlap in both enzymatic activity and neurobiological function between spastin and katanin suggests that *katna1* could be a potential disease-modifying factor and account for some of the variation in severity and age of onset seen in *SPAST* HSP cases. The phenotypic enhancement of motor axon outgrowth defects observed in embryos injected with both *spast* and *katna1* morpholinos implies that the microtubule-severing activities of each protein play related roles in axon outgrowth in vivo. Although caution should be shown when interpreting the combined effect of two hypomorphic states, our data clearly demonstrate that levels of katanin activity can influence the motor axon phenotype caused by reduced spastin activity. This finding suggests that the variation in severity and/or age of onset seen in *SPAST* HSP cases could, at least in part, be determined by levels of katanin activity. Other microtubule-severing proteins such as those encoded by *KATNAL1* and *KATNAL2* might also act as modifiers of spastin function.

Our findings are consistent with the hypothesis of templated nucleation from severed microtubules in axons (Roll-Mecak and Vale, 2006). Although EB3-GFP was found to localise to anterograde-moving comet-like structures in axons of control zebrafish neurons in vivo (Fig. 3A), this behaviour was in marked contrast to the situation in axons of *spast*- and *katna1*-morphant embryos, where EB3-GFP was still detectable in truncated axons, but the comet-like

Table 3. Effect of nocodazole on spinal motor neuron axon outgrowth in *spast*-morphant embryos[a]

	Severity (%)			
Treatment	**0**	**1**	**2**	**3**
Untreated (n=46)	89.1	10.9	0	0
spg4atg1 only (n=74)	0	33.8	63.5	2.7
spg4atg1 + DMSO (n=43)	0	39.5	53.5	7.0
spg4atg1 + 0.1 µg/ml nocodazole (n=78)	0	6.4	83.3	10.3
spg4atg1 + 0.3 µg/ml nocodazole (n=48)	0	0	77.1	22.9
spg4atg1 + 0.5 µg/ml nocodazole (n=73)	0	1.4	67.1	31.5
spg4atg1 + 1.0 µg/ml nocodazole (n=80)	0	0	65.0	35.0

[a]Data pooled from three independent experiments.

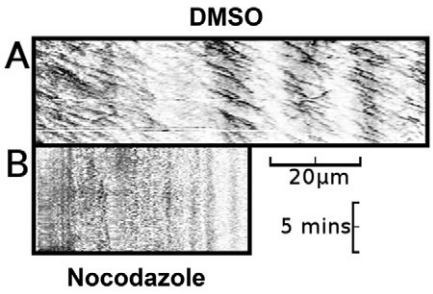

Fig. 5. Nocodazole-treated embryos lack both EB3-GFP puncta and axonal movement of EB3-GFP. (A) Kymograph of an axon made from a 10-minute time-lapse recording of a neuron from a DMSO-vehicle-treated embryo, demonstrating predominantly anterograde movement of discrete puncta of EB3-GFP fluorescence (*n*=16). (B) Kymograph of an axon made from a 10-minute time-lapse recording of a neuron from a nocodazole-treated embryo, demonstrating absence of axonal movement of EB3-GFP fluorescence (*n*=10). Horizontal scale bar: 20 μm, vertical scale bar: 5 minutes. See supplementary material Movies 7 and 8.

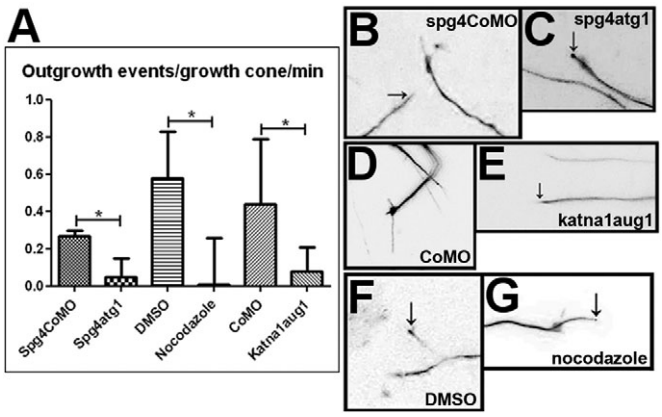

Fig. 6. Disruption of microtubule dynamics reduces growth cone activity in the zebrafish embryonic CNS. An outgrowth event was scored as a continuous period of growth of a single process from the distal end of an axon. Scoring was carried out on 10-minute time-lapse recordings and the mean number of outgrowth events per growth cone was calculated. (A) The number of outgrowth events occurring per growth cone per minute is reduced by knockdown of *spast* (*P*=0.0179), knockdown of *katna1* (*P*=0.025) and treatment with nocodazole (*P*=0.0155). Values were calculated using a two-tailed Student's *t*-test assuming unequal variance. (B-G) Frames taken from 10-minute time-lapse recordings of the distal part of EB3-GFP-expressing neurons in live zebrafish embryos. When embryos were injected with spastin control morpholino (B), standard control morpholino (D), or treated with DMSO (F), growth cones were highly motile and rapid outgrowth and branching of GFP-labelled processes (arrows in B and F) was observed. When embryos were injected with *spast* (C) or *katna1* (E) morpholinos, or treated with nocodazole (G), growth cone activity was greatly reduced. In some cases, the tips of immobile processes (arrows in C and G) were brightly labelled with an accumulation of EB3-GFP. Scale bars: 10 μm. See supplementary material Movies 9-14.

structures were completely absent (Fig. 3B-E). Kymograph analysis demonstrated that there was still a generalised anterograde 'drift' of diffuse EB3-GFP fluorescence in both *spast*- and *katna1*-morphant embryos. This continued anterograde movement of small EB3-GFP-positive particles when spastin and katanin are knocked down could be explained by passive diffusion or transport of free EB3-GFP distally, or uncoordinated movement of individual dynamic microtubules in an anterograde direction. These results suggest that the microtubule-severing activity of spastin and katanin promotes the concerted, coordinated anterograde growth and/or movement of microtubule plus-ends that are decorated with +TIPS such as EB3. This leads to a model in which we suggest that a certain level of microtubule severing facilitates concerted growth of microtubules by creating many co-aligned new plus-ends in one place, the growth of which is then coordinately promoted within the axon (Fig. 8). This hypothesis is supported by evidence that spastin can bundle microtubules in vitro (Salinas et al., 2005), and that bundled microtubules are required for maintenance of axons (Erturk et al., 2007). Owing to the highly dynamic nature of the microtubule network, this concerted growth might ensure that enough microtubules arrive at sites of growth and branching at the same time to provide the physical force to move the tip of the growth cone or branch point forward. Indeed, the fact that the reduction in the number of outgrowth events at the growth cone is equally severe when microtubule severing is reduced and when microtubules are destabilised by nocodazole treatment (Fig. 6) indicates that microtubule severing is vitally important for extension of growth cone filopodial processes. The recent finding by Riano et al. (Riano et al., 2009) that the velocity of EB3-GFP comets is reduced by small interfering RNA (siRNA) knockdown of spastin in the neurites of in vitro cultured neuroblastoma × spinal cord 34 (NSC34) cells further supports the idea that microtubule severing is required for concerted anterograde movement or growth of microtubules. The authors suggest that the decrease in comet velocity observed results from an increased proportion of longer and older microtubules, which can more readily accumulate stabilising post-translational modifications, making them resistant to turnover. The complete loss of comets when spastin is knocked down that we report here could represent a higher sensitivity of zebrafish neurons to loss of microtubule severing, as compared with the neurites of neuron-like cells in vitro, or reflect differences in the efficiencies of morpholino- and siRNA-mediated

Table 4. Effect of simultaneous *katna1* and *spast* knockdown on spinal motor neuron axon outgrowth[a]

	Severity (%)			
Treatment	**0**	**1**	**2**	**3**
Uninjected (*n*=103)	89.3	4.9	5.8	0
1.2 pmol CoMO (*n*=101)	81.2	12.9	5.0	0.9
0.3 pmol spg4atg1 (*n*=104)	3.8	40.4	52.9	2.9
0.9 pmol katna1aug1 (*n*=85)	10.6	50.6	27.1	11.8
0.3 pmol spg4atg1 + 0.9 pmol katna1aug1 (*n*=96)	3.1	5.2	33.3	58.3

[a]Data pooled from three independent experiments.

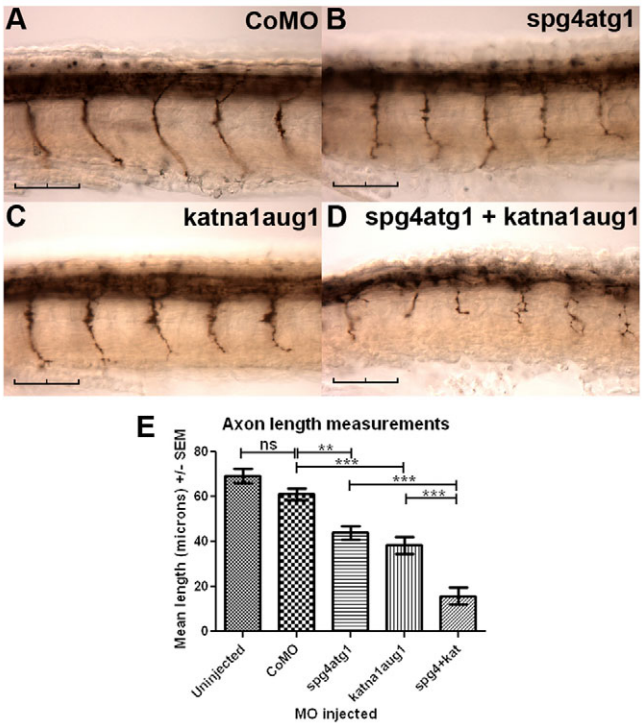

Fig. 7. Simultaneous knockdown of *katna1* and *spast* enhances phenotypic severity. Immunostaining with znp-1 demonstrates that embryos co-injected with 0.3 pmol of spg4atg1 and 0.9 pmol of katna1aug1 morpholinos showed far more severe defects in spinal motor axon outgrowth (D) than embryos injected with either 0.3 pmol of spg4atg1 (B) or 0.9 pmol of katna1aug1 (C) alone. (A) Control embryo injected with 1.2 pmol of a control morpholino. (E) Quantification of mean spinal motor axon length in morpholino-injected embryos. Statistical significance was determined using ANOVA with Bonferroni's multiple comparison test: ns, not significant; $^{**}P<0.01$; $^{***}P<0.001$. Scale bars: 50 µm.

knockdown. More recently, Qiang et al. reported that overexpression of spastin in rat hippocampal neurons increased the number of EB3 comets, but had no effect on mean comet velocity (Qiang et al., 2009). The effect of spastin knockdown on comet number and velocity was not reported in this study.

As was observed when spastin and katanin expression was knocked down, we found that treatment of embryos with nocodazole inhibited axonal outgrowth of spinal motor neurons. However, the results obtained from the live imaging analysis also showed that destabilisation of microtubules with nocodazole prevented all growth and movement of microtubules, because anterograde movement of all EB3-GFP fluorescent material was lost in nocodazole-treated embryos. This observation contrasts with the situation in *spastin* and *katna1* morphants, where a background level of anterograde movement of small EB3-GFP-positive particles could be observed even though comet formation was completely inhibited. The difference between the phenotypes of nocodazole-treated embryos and *spast* or *katna1* morphants suggests that loss of microtubule-severing activity might primarily affect the organisation, possibly bundling, of dynamic microtubules, rather than their anterograde movement. We found that administration of nocodazole to *spast*-morphant embryos did not ameliorate the motor axon outgrowth defects caused by inhibition

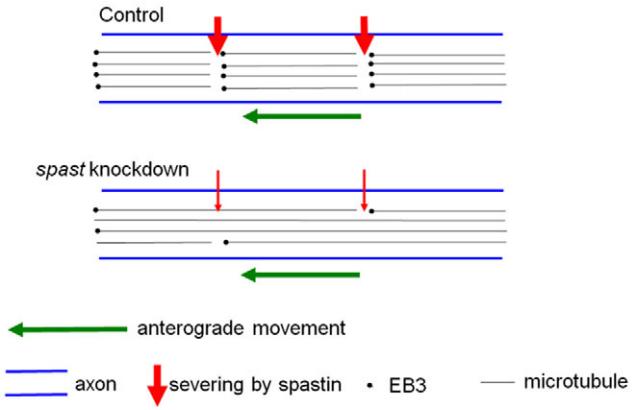

Fig. 8. Hypothesis for how microtubule severing by spastin and katanin promotes concerted growth of microtubules. Microtubule severing is required to allow concerted growth of microtubules by creating many new plus-ends in the same place, which then extend down the axon together, giving the appearance of a comet.

of *spast* function. Interestingly, this result contrasts with observations in Drosophila models of *SPAST* HSP, where microtubule-destabilising drugs ameliorated both synaptic abnormalities at larval neuromuscular junctions and adult motor defects caused by loss of spastin function (Orso et al., 2005; Trotta et al., 2004). It is unclear how the different effects arise in the different models, but one possibility is that both microtubules and the microtubule-severing activity of spastin perform mechanistically distinct functions in neuromuscular synapses and growing axons. For example, at the neuromuscular junction, stable microtubules could promote neurotransmission by facilitating trafficking of synaptic vesicles. If so, then reduced spastin function would be expected to enhance both microtubule stability and neurotransmission at the Drosophila neuromuscular junction, as was observed. Moreover, administration of the microtubule-destabilising drug nocodazole would be predicted to suppress neurotransmission, as was also observed. By contrast, if growth of axons and motility of growth cones require dynamic microtubules, then each of these behaviours would be dependent on spastin for production of new microtubule plus-ends, from which growth could then occur. Similarly, disassembly of microtubules by nocodazole, like inhibition of spastin function, would also be expected to impair axon outgrowth and growth cone motility, as was observed in our experiments. Thus, if defective microtubule dynamics in axons and growth cones is a contributory cause of HSP in *SPAST* cases, then effective therapy might require identification of compounds that stimulate microtubule dynamics.

In conclusion, our results demonstrate that the zebrafish embryo provides a powerful model system for in vivo analysis of microtubule dynamics that is amenable to both genetic and chemical manipulation. Our results also suggest that perturbation of axonal microtubule dynamics might contribute to axonal degeneration in HSP, and that the zebrafish embryo could be useful for identifying compounds that modulate microtubule dynamics in vivo, some of which might be beneficial for treatment of HSP. Although cell culture, fly and mouse models of HSP have been developed, the zebrafish embryo provides new opportunities to combine in vivo analysis of disease mechanisms with

pharmacological manipulations. These practical advantages are not limited to the study of HSP and suggest that further research with zebrafish could help to improve understanding and treatment of a variety of other neurological disorders.

METHODS

Zebrafish maintenance

LWT and AB zebrafish were used for this study, and embryos were obtained by natural mating. All procedures involving experimental animals were performed in compliance with local animal welfare laws, guidelines and policies.

Drug treatments

Stock solutions of nocodazole and vinblastine were prepared in and diluted with DMSO. Drugs in DMSO, and DMSO alone, were added directly to E3 medium containing embryos from 10 or 24 hpf.

DNA constructs

Cloning of human EB3 into pEGFP-N1 is described elsewhere (Stepanova et al., 2003). EB3-GFP cDNA was excised using *Hind*III and *Sma*I, and placed under control of the Xenopus neural-specific β-tubulin (NBT) promoter by ligating into an NBT:MAPT-GFP vector (constructed by Enrique Amaya, University of Manchester, Manchester, UK; a gift from Chi-Bin Chien, University of Utah Medical Center, UT) from which the MAPT-GFP cDNA had been excised using *Hind*III and *Sna*BI.

Microinjection of morpholinos and DNA constructs

All morpholinos were designed by and purchased from Gene Tools, LLC (Philomath, OR). To block *katna1* function, morpholino antisense oligonucleotides (MOs) were designed against the initiating AUG of *katna1* (katna1aug1, 5′-TCATCCTGTAAGTTAAAGTGGTCAG-3′) and against the exon-4–intron-4 splice donor site of *katna1* (katna1e4i4, 5′-CACAGATCTTCCTCACCTTGTCTTC-3′). The *spast* AUG-blocking MO (spg4atg1), *spast* splice-blocking MO (spg4e7i7) and *spast* control MO (spg4CoMO) are described elsewhere (Wood et al., 2006). A standard control MO (CoMO) that targets human β-globin pre-mRNA and a morpholino that targets zebrafish p53 were also used. NBT:EB3-GFP was linearised with *Xba*I prior to injection. Morpholinos (0.3-0.9 mM) and DNA (150 ng/μl) were resuspended in water with Phenol Red, and 2 nl microinjected into one-cell embryos using a Narishige IM-300 microinjector. Embryos were maintained at 28.5°C in E3 medium and dechorionated with fine forceps prior to live imaging or fixation.

Immunoblotting

Total protein was prepared from zebrafish embryos at 29 hpf. Embryos were deyolked by pipetting up and down in deyolking buffer (55 mM NaCl, 1.8 mM $NaHCO_3$), then washed once in wash buffer (110 mM NaCl, 3.5 mM KCl, 2.7 mM $CaCl_2$, 10 mM Tris-HCl pH 8.5). Deyolked embryos were prepared for SDS-PAGE by heating for 5 minutes at 100°C in 4 μl SDS-PAGE sample buffer per embryo. SDS-PAGE and immunoblotting were performed using standard procedures. Immunoblots were probed for spastin using S51 (Errico et al., 2004), katna1 using ab67206 (abcam, Cambridge, UK), and α-tubulin using DM1A (Sigma, Poole, UK).

TRANSLATIONAL IMPACT

Clinical issue

The hereditary spastic paraplegias (HSP) are a collection of neurodegenerative disorders characterised by progressive weakness and spasticity of the legs. They are caused by developmental failure or degeneration of motor axons, or nerve fibres, in the corticospinal tract, and are an important cause of permanent disability. Around 40% of autosomal dominant cases of HSP are caused by mutations in the *SPAST* gene. HSP cases show highly variable age of onset and severity, both between and within families, and haploinsufficiency for *SPAST* is the likely mechanism in most cases.

Current treatments to provide symptomatic relief for HSP include muscle relaxants to relieve spasticity, and physical therapy to maintain muscle strength and range of movement. However, these treatments do not alter or slow the disease, and the development of effective therapies has been hampered by a lack of knowledge regarding the molecular mechanisms underlying axonal degeneration.

Results

Previous work has shown that spastin, the *SPAST* gene product, shares homology with the p60 subunit of katanin, and both proteins have been shown to be ATP-dependent microtubule-severing proteins. Microtubules, components of the cell's cytoskeleton, are fundamentally important for the correct outgrowth of axons, but how microtubule-severing activities might relate to axonal degeneration in HSP is unclear. This study uses confocal time-lapse imaging in the zebrafish embryonic CNS to demonstrate that both spastin and katanin are required in axons for the formation of forward-moving dynamic microtubules, and also at the growth cone, the specialised guidance structure at the axon's growing tip. The effects of lowering the levels of spastin and katanin, mimicking haploinsufficiency, were monitored in embryonic neurons using a fluorescent protein as a marker for the growing microtubules. Reduced expression of either spastin or katanin severely impaired formation of dynamic microtubules and inhibited outgrowth of axons and growth cone motility. The microtubule-destabilising drug nocodazole also abolished microtubule dynamics, suppressed growth cone motility and enhanced the severity of the phenotypes caused by reduced spastin expression in the embryos.

Implications and future directions

These results reveal crucial functions for microtubule-severing proteins in neuronal development, through their roles in dynamic microtubule formation, axonal outgrowth and growth cone protrusive activity. *SPAST* mutations might cause depletion of the pool of dynamic microtubules in neurons, leading to a failure to maintain long axons and the axonal transport machinery within, which could explain the distal axonopathies that are observed in HSP patients. Future studies will aim to identify compounds that modulate microtubule dynamics, which might be of therapeutic value for treatment of HSP.

doi:10.1242/dmm.006197

RT-PCR

Total RNA was isolated from zebrafish embryos at 28 hpf using TRIZOL reagent (Invitrogen). First-strand cDNA was synthesised using SuperSript II (Invitrogen), and a region of *katna1* spanning exons 2-6 (nt 243-888) was amplified using the following primers: 5′-AGCTCTGCGGTGGTCTGTTATC-3′ and 5′-TCCATGGGCGTCTTATTCCTT-3′.

Immunostaining of embryos and analysis of axon outgrowth defects

Embryos were fixed with 4% paraformaldehyde at 4°C overnight and immunohistochemistry was performed using standard procedures (Schulte-Merker, 2003). Motor axons were immunostained using monoclonal antibody znp-1 (Developmental Studies Hybridoma Bank, University of Iowa, IA; 1:2000 dilution).

Primary antibody binding was visualised using a VECTASTAIN Elite ABC kit (Vector Laboratories, Burlingame, CA). For qualitative analysis of motor axon outgrowth defects, spinal motor neuron fascicles in ten anterior somites on both sides of the spinal cord were examined using a stereomicroscope and axon outgrowth was scored as follows: 0 = normal, all axons normal; 1 = mild defect, less than 10% of axons aberrantly branched or truncated; 2 = moderate defect, 10-50% of axons aberrantly branched or truncated; 3 = severe defect, more than 50% of axons aberrantly branched or truncated. For quantitative analysis of axon outgrowth defects, spinal motor axons were measured using ImageJ (Rasband, 1997-2007) and an axon measurement plug-in designed and written by R.B. to partially automate the analysis. Mean lengths were calculated and subjected to one-way analysis of variance (ANOVA) with Bonferroni's multiple comparison test. Statistical analysis was performed using GraphPad Prism software.

Live imaging and analysis of EB3-GFP movements

Embryos (28 hpf) were mounted in 1% low-melting-point agarose containing 0.03% tricaine. Time-lapse recordings of the growth cones and axons of individual neurons were made using an Olympus FV1000 confocal microscope with a 60× water immersion objective (NA 1.2) and a 2× digital zoom applied. *Z*-stacks were taken every 6 seconds over a 10-minute period. Stacks of images were *z*-projected and processed using ImageJ (Rasband, 1997-2007). Stacks were aligned using the stackreg plug-in (Thévenaz et al., 1998) and axons were straightened using the straighten plug-in (Kocsis et al., 1991). Kymographs were made using the kymograph plug-in designed and written by R.B. to partially automate kymograph production from straightened stacks and optimise their appearance.

ACKNOWLEDGEMENTS

We are grateful to Tanya Whitfield, Andrew Grierson and Philip Ingham for sharing fish, experimental materials and other reagents, and to Claire Allen, Lisa Gleadall, Susanne Surfleet and Matthew Green for fish care. We are also grateful to Elena Rugarli, University of Cologne, for the kind gift of the anti-spastin S51 antibody. Funding from the MRC to support the Centre for Developmental and Biomedical Genetics (Grants G0400100 and G0700091 to Philip Ingham) is gratefully acknowledged. The core BMS-MBB Light Microscopy Facility was funded by a grant from The Wellcome Trust (GR077544AIA). This work was funded by a research grant from the Spastic Paraplegia Foundation (http://sp-foundation.org/index.html) and a Medical Research Council PhD studentship to R.B. Deposited in PMC for release after 6 months.

COMPETING INTERESTS

The authors declare no competing financial interests.

AUTHOR CONTRIBUTIONS

R.B., V.T.C. and J.D.W. conceived and designed the experiments. R.B., J.A.L. and J.D.W. performed the experiments. R.B., V.T.C., J.A.L. and J.D.W. analysed the data. R.B., V.T.C. and J.D.W. wrote the paper.

SUPPLEMENTARY MATERIAL

Supplementary material for this article is available at http://dmm.biologists.org/lookup/suppl/doi:10.1242/dmm.004002/-/DC1

Received 27 June 2009; Accepted 27 May 2010.

REFERENCES

Ahmad, F. J., Yu, W., McNally, F. J. and Baas, P. W. (1999). An essential role for katanin in severing microtubules in the neuron. *J. Cell Biol.* **145**, 305-315.

Charvin, D., Cifuentes-Diaz, C., Fonknechten, N., Joshi, V., Hazan, J., Melki, J. and Betuing, S. (2003). Mutations of SPG4 are responsible for a loss of function of spastin, an abundant neuronal protein localized in the nucleus. *Hum. Mol. Genet.* **12**, 71-78.

Crosby, A. H. and Proukakis, C. (2002). Is the transportation highway the right road for hereditary spastic paraplegia? *Am. J. Hum. Genet.* **71**, 1009-1016.

Durr, A., Davoine, C. S., Paternotte, C., von Fellenberg, J., Cogilinicean, S., Coutinho, P., Lamy, C., Bourgeois, S., Prud'homme, J. F., Penet, C. et al. (1996). Phenotype of autosomal dominant spastic paraplegia linked to chromosome 2. *Brain* **119**, 1487-1496.

Errico, A., Ballabio, A. and Rugarli, E. I. (2002). Spastin, the protein mutated in autosomal dominant hereditary spastic paraplegia, is involved in microtubule dynamics. *Hum. Mol. Genet.* **11**, 153-163.

Errico, A., Claudiani, P., D'Addio, M. and Rugarli, E. I. (2004). Spastin interacts with the centrosomal protein NA14, and is enriched in the spindle pole, the midbody and the distal axon. *Hum. Mol. Genet.* **13**, 2121-2132.

Erturk, A., Hellal, F., Enes, J. and Bradke, F. (2007). Disorganized microtubules underlie the formation of retraction bulbs and the failure of axonal regeneration. *J. Neurosci.* **27**, 9169-9180.

Evans, K. J., Gomes, E. R., Reisenweber, S. M., Gundersen, G. G. and Lauring, B. P. (2005). Linking axonal degeneration to microtubule remodeling by Spastin-mediated microtubule severing. *J. Cell Biol.* **168**, 599-606.

Karabay, A., Yu, W., Solowska, J. M., Baird, D. H. and Baas, P. W. (2004). Axonal growth is sensitive to the levels of katanin, a protein that severs microtubules. *J. Neurosci.* **24**, 5778-5788.

Kocsis, E., Trus, B. L., Steer, C. J., Bisher, M. E. and Steven, A. C. (1991). Image averaging of flexible fibrous macromolecules: the clathrin triskelion has an elastic proximal segment. *J. Struct. Biol.* **107**, 6-14.

Lowery, L. A. and Van Vactor, D. (2009). The trip of the tip: understanding the growth cone machinery. *Nat. Rev. Mol. Cell Biol.* **10**, 332-343.

McDermott, C. J., Grierson, A. J., Wood, J. D., Bingley, M., Wharton, S. B., Bushby, K. M. and Shaw, P. J. (2003). Hereditary spastic paraparesis: disrupted intracellular transport associated with spastin mutation. *Ann. Neurol.* **54**, 748-759.

Orso, G., Martinuzzi, A., Rossetto, M. G., Sartori, E., Feany, M. and Daga, A. (2005). Disease-related phenotypes in a Drosophila model of hereditary spastic paraplegia are ameliorated by treatment with vinblastine. *J. Clin. Invest.* **115**, 3026-3034.

Patrono, C., Casali, C., Tessa, A., Cricchi, F., Fortini, D., Carrozzo, R., Siciliano, G., Bertini, E. and Santorelli, F. M. (2002). Missense and splice site mutations in SPG4 suggest loss-of-function in dominant spastic paraplegia. *J. Neurol.* **249**, 200-205.

Qiang, L., Yu, W., Liu, M., Solowska, J. M. and Baas, P. W. (2009). Basic fibroblast growth factor elicits formation of interstitial axonal branches via enhanced severing of microtubules. *Mol Biol. Cell* **21**, 334-344.

Rasband, W. S. (1997-2007). ImageJ, U. S. National Institutes of Health, Bethesda, Maryland, USA, http://rsb.info.nih.gov/ij/.

Reid, E. (2003). Science in motion: common molecular pathological themes emerge in the hereditary spastic paraplegias. *J. Med. Genet.* **40**, 81-86.

Riano, E., Martignoni, M., Mancuso, G., Cartelli, D., Crippa, F., Toldo, I., Siciliano, G., Di Bella, D., Taroni, F., Bassi, M. T. et al. (2009). Pleiotropic effects of spastin on neurite growth depending on expression levels. *J. Neurochem.* **108**, 1277-1288.

Robu, M. E., Larson, J. D., Nasevicius, A., Beiraghi, S., Brenner, C., Farber, S. A. and Ekker, S. C. (2007). p53 activation by knockdown technologies. *PLoS Genet.* **3**, e78.

Roll-Mecak, A. and Vale, R. D. (2005). The Drosophila homologue of the hereditary spastic paraplegia protein, spastin, severs and disassembles microtubules. *Curr. Biol.* **15**, 650-655.

Roll-Mecak, A. and Vale, R. D. (2006). Making more microtubules by severing: a common theme of noncentrosomal microtubule arrays? *J. Cell Biol.* **175**, 849-851.

Salinas, S., Carazo-Salas, R. E., Proukakis, C., Cooper, J. M., Weston, A. E., Schiavo, G. and Warner, T. T. (2005). Human spastin has multiple microtubule-related functions. *J. Neurochem.* **95**, 1411-1420.

Schulte-Merker, S. (2003). Looking at zebrafish embryos. In *Zebrafish: a Practical Approach* (ed. C. Nusslein-Volhard and R. Dahm), pp. 39-58. Oxford: Oxford University Press.

Stepanova, T., Slemmer, J., Hoogenraad, C. C., Lansbergen, G., Dortland, B., De Zeeuw, C. I., Grosveld, F., van Cappellen, G., Akhmanova, A. and Galjart, N. (2003). Visualization of microtubule growth in cultured neurons via the use of EB3-GFP (end-binding protein 3-green fluorescent protein). *J. Neurosci.* **23**, 2655-2664.

Thévenaz, P., Ruttimann, U. E. and Unser, M. (1998). A pyramid approach to subpixel registration based on intensity. *IEEE Trans. Image Process.* **7**, pp. 27-41.

Trotta, N., Orso, G., Rossetto, M. G., Daga, A. and Broadie, K. (2004). The hereditary spastic paraplegia gene, spastin, regulates microtubule stability to modulate synaptic structure and function. *Curr. Biol.* **14**, 1135-1147.

Wood, J. D., Landers, J. A., Bingley, M., McDermott, C. J., Thomas-McArthur, V., Gleadall, L. J., Shaw, P. J. and Cunliffe, V. T. (2006). The microtubule-severing protein Spastin is essential for axon outgrowth in the zebrafish embryo. *Hum. Mol. Genet.* **15**, 2763-2771.